testing, respectively. The uteruses and decalcified femurs were then embedded in paraffin and sectioned for histopathological examination.
Results: Compared with the Sham group, the uterus indexes reduced significantly in OVX and ICT mice, with no significant difference between OVX and ICT mice. Histopathological examination of uterus showed a thinned endometrium with atrophic glands in OVX and ICT mice. Micro-CT analysis showed that the bone mineral density, bone volume/tissue volume, trabecular number and trabecular thickness of the 5th lumbar vertebrae all decreased significantly, and the trabecular separation increased in OVX mice. Mechanical testing showed that the biomechanical properties of the 5th lumbar vertebrae in OVX mice reduced, including the sectional elastic modulus, the maximum failure force and the energy absorbed until failure. Histopathological examination of femurs showed thin and spaced trabecular bone accompanied by increased bone marrow fat content in OVX mice. However, these osteoporotic phenotypes were rescued in ICT mice.
Conclusion: Icaritin can prevent OVX-induced osteoporosis in mice, without hyperplastic effect on uterus.
Acknowledgements
This work was supported by the grants from NSFC (No. 81200650 and 81302782).

IBDW2014-00107-F0037
INVESTIGATION OF HIERARCHICAL POROUS MICROSTRUCTURE OF SHANKBONE

B. Chen, D. Yin, S. Lin
College of Aerospace Engineering, Chongqing University, Chongqing 400044, China

Introduction and aims: Bone possesses high fracture strength and toughness. Simultaneously, it is also relatively light. The excellent mechanical and physical properties of the bone are highly related to its elaborate microstructure refined by nature over many centuries. The detailed research on bone microstructure and the relationship between the microstructure and the properties of the bone can reveal the mechanism of strength and toughness as well as light-weight of the bone.
Methods: In this study, the hierarchical porous microstructure of a shankbone was first analyzed by a scanning electron microscope (SEM) under different scales and directions. Then an image processing with a higher gray-scale resolution was used to analyze the SEM images of the porous microstructure of the bone under different scales. The porosity at different locations of the bone under different directions was identified. Lastly, the number and size of pores and density of the bone along different directions and under different scales were investigated by a MATLAB program.
Results: It was revealed that the bone was a porous bioceramics composite with particularly porous microstructure which varied by different scales, location and direction. It was indicated that the number and size of pores and density of the bone varied with the observed locations, directions and scales.
Conclusion: The polynomial expressions for the number and size of the pore and density of the bone are fitted from the relation curves between the number and size of the pores and density of the bone and the locations, directions and scales, which reveals the hierarchical porous microstructural characteristic of the bone.

IBDW2014-00108-F0038
RELATIONSHIP BETWEEN MICROSTRUCTURE AND MECHANICAL BEHAVIOR OF CORTICAL BONE

B. Chen, S. Lin, D. Yin
College of Aerospace Engineering, Chongqing University, Chongqing 400044, China

Introduction and aims: The mechanical behaviors of the bone, such as fracture susceptibility, are closely related to the microstructure of the bone. Therefore, the investigation on the relationship between the mechanical behavior and the microstructure of the bone is important. This investigation used the experiment and models of microscopic mechanics. The combination of the experiment and analytical models at microscopic scale could provide a fair understanding of the mechanical behavior of the bone.
Methods: In this work, the observation of scanning electron microscope, nanoindentation technique, hierarchical-model analysis and finite element computation at microscopic scale were used to investigate the relationship between the mechanical behavior of a cortical bone and its microstructure, such as its porosity, density and the direction of the hydroxyapatite-fiber sheets. In the hierarchical-model analysis, the osteons in the cortical bone were first considered as hollow fibers and the interstitial bone as matrix, and then the osteons were further taken as a combination of many hydroxyapatite-fiber plies. Each fiber ply had different direction and modulus that provided different contributions to the mechanical properties of the bone. The porosity in the bone as well as the direction of the hydroxyapatite-fiber sheets in the osteons were modeled explicitly based on the images of the scanning electron microscope and X-ray diffraction. Computational results were obtained by applying uniform macroscopic stress to the boundaries of the microscopic model of the bone.
Results: The prediction of the macroscopic mechanical property corresponded reasonably well with the experimental data.
Conclusion: The relationship between the mechanical behavior and the microstructure of the bone is discussed in detail.

IBDW2014-00109-F0039
TISSUE MINERAL DENSITY DEPENDENT MECHANICAL PROPERTIES OF INDIVIDUAL TRABECULA PLATES AND RODS DO NOT DIFFER IN ANATOMIC DIRECTIONS BUT INDIVIDUAL TRABECULAR DIRECTIONS

Yue Eric Yu, Ji Wang, Bin Zhou, X. Edward Guo
Department of Biomedical Engineering, Columbia University, NY, USA

Introduction and aims: Trabecular bone, susceptible to osteoporosis, consists of individual trabecular plates and rods, which are distributed distinctly along the longitudinal, transverse, or oblique anatomic directions of the skeleton (Fig.1). In each anatomic direction, mechanical properties of bone tissue are also expected to differ in (axial) or against (lateral) the direction of individual trabeculae, i.e., anisotropic mechanical properties. However, anisotropic mechanical properties of individual trabeculae along various anatomic directions are currently unclear. **Objectives** of this study were 1) to measure anisotropic tissue modulus and tissue mineral density (TMD) of individual trabeculae; 2) to examine their dependence on trabecular types and anatomic directions; and 3) to determine the relationship between anisotropic tissue modulus and TMD of individual trabeculae.
Methods: Twelve cylindrical human trabecular bone samples of proximal femurs were imaged with hydroxyapatite density calibration phantoms at 25μm resolution by micro-computed tomography (μCT). Individual trabecular types and their anatomic directions were determined using individual trabeculae segmentation (ITS) technique. On the embedded samples, microindentation tests were performed under wet condition on both axial and lateral cross-sections (Fig 1.C) of selected plates and rods in longitudinal (L), transverse (T), and oblique (O) directions, respectively (Fig 1.D). The point-by-point registered grayscale values of the μCT image at the indentation sites were converted to TMD using calibration phantoms.
Results: The tissue modulus and the co-localized TMD of trabecular plates were significantly higher than those of trabecular rods (Fig. 2A, B). The axial tissue modulus of individual trabeculae was significantly higher than the lateral tissue modulus (Fig. 2C). The tissue modulus correlated strongly with TMD. These correlations did not differ significantly between plates and rods or between different anatomic directions. However, the correlation of axial modulus was significantly different from that of lateral modulus (Fig. 2D).
Conclusion: We measured anisotropic elastic modulus of individual trabecular plates and rods of different anatomic directions. Surprisingly, the heterogeneous tissue modulus correlated with TMD similarly regardless of trabecular types and anatomic directions. The correlation only differs

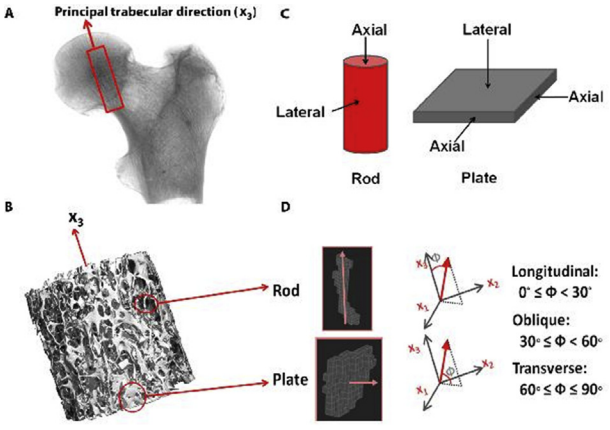

A. X-ray radiography illustration of the principle trabecular direction of femoral neck trabecular bone
B. μCT illustration of the trabecular structure of a cylinder sample corresponding to the red box in Fig.1 A
C. Axial and lateral directions of trabecular plates and rods
D. Classification of anatomic directions of plates and rods

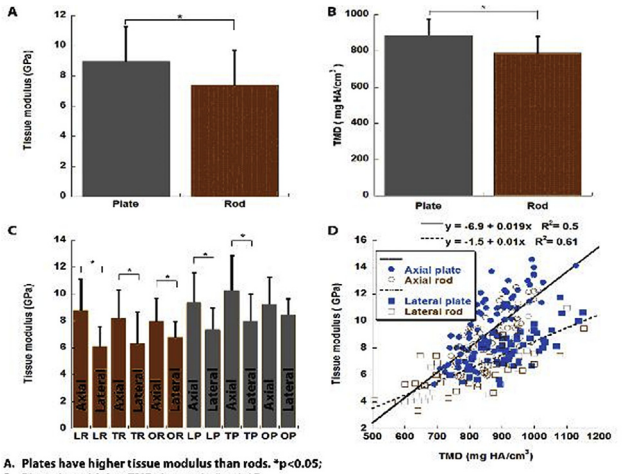

A. Plates have higher tissue modulus than rods. *p<0.05;
B. Plates have higher TMD than rods. *p<0.05
C. Tissue modulus in axial direction is higher than in lateral direction. *p<0.05. P and R denote plate and rod. L, T, O denote longitudinal, transverse and oblique. (p=0.53 for OP axial vs. OP lateral)
D. Tissue modulus closely correlates with TMD. However, the correlations differ between axial and lateral directions, *p<0.05

between the axial and lateral trabecular directions. It remains to be determined how this heterogeneous anisotropic tissue property plays a role in whole bone mechanical competence.

IBDW2014-00111-F0040
AN INTELLIGENT PIPELINE FOR DESIGNING PERSONALIZED ORTHOPEDIC CASTS

Defeng Wang [a], Ka Ming Fung [a], Lin Shi [b]
[a]*Division of Imaging Informatics, Department of Imaging and Interventional Radiology, The Chinese University of Hong Kong, Shatin, NT, Hong Kong*
[b]*Department of Medicine and Therapeutics, The Chinese University of Hong Kong, Shatin, NT, Hong Kong*

Introduction and aims: Bone fracture may happen as a result of traumatic injuries during traffic accidents or sport activities. For every thousand people in Hong Kong, almost 4.5 people suffered from a bone fracture after injury and about 86.7% of the fractures sustained at the limbs of the patients (HKSAR-Government, 2011). Traditional orthopedic casts have been used to mold the soft tissue to the fractured bones for more than 150 years (Large, 2001). The principle of this treatment is to give extra supports and immobilize the body parts to allow the bones to heal by providing sufficient support. A new mesh-like 3D printed cast design was introduced previously. This porous structure could improve ventilation and avoid dry skins and rashes at which the cast is applied. Fabrication of such design does not rely on the craftsmanship of the practitioners. Also, rapid production is beneficial when treating patients with size-changing injured limbs which requires frequent cast replacement. We propose to develop a user-friendly automatic pipeline for designing 3D printed orthopedic casts based on geometric and structural analyses.
Methods: With the help of radiographic imaging techniques, such as MR, CT, or 3D scanners, precise 3D models of the body parts could be obtained. Our proposed algorithm would calculate the sizes and shapes of casts based on the models to ensure the casts are body-fitting. With an optimization algorithm, a mesh-like framework of the cast could be determined. To ensure the performance of the cast, stress analyses would be conducted. The results could assist in acquiring the minimal thickness at different locations of the cast in order to balance its effectiveness and environmental friendliness. An interactive feature will be implemented to allow medical specialists to define regions that extra supports are required according to the patients' conditions. When the optimized cast is accomplished, it could be sent for fabrication using 3D printers.
Results: The advantages of using 3D printed cast include rapidness of production, objectiveness, precision and wide range of materials. The newly proposed design of orthopedic cast could provide a better user experience to the patients. The obstacles are its complex structure and lack of evidence for its reliability.
Conclusion: In summary, Our proposed cast design software could assist medical professionals to utilize the advantageous 3D printing technology for producing the casts without time consuming training. The stress analysis in our pipeline could quantitatively determine the optimal geometry of the casts and ensure its workability.
References
HKSAR-Government. (2011). Fracture Overview. Non-Communicable Diseases Watch Volume 4(Number 7).
Large, P. (2001). A 'new focus' in casting—an introduction to the concepts of focus rigidity casting. Journal of Orthopaedic Nursing, 5(4), 176-179.

IBDW2014-00113-F0041
CULTIVATION OF BONE MARROW STROMAL STEM CELLS (BMSCS) IN POROUS TANTALUM AND ITS SCAFFOLD

Xiaowei Wei, Dewei Zhao, Benjie Wang, Wei Wang, Kai Kang, Hui Xie, Fan Yang
Department of Orthopaedic Laboratory, Zhongshan Hospital of Dalian University, PR China

Porous tantalum metal, a new low modulus metal with characteristic appearance similar to cancellous bone, is currently available for use in several orthopedic applications. Reticulated vitreous carbon (RVC) can provide three-dimensional pore structure and serve as an ideal scaffold of porous tantalum. Also, as we all know, autologous bone marrow stromal stem cells (BMSCs) can mobilize for bone defect reconstruction. In this study, domestic RVC and porous tantalum were tested in vitro for biocompatibility with BMSCs adhesion and proliferation. BMSCs were obtained from Beagle dogs, cultured and identified by immunofluorescence staining and flow cytometry with CD90, CD44 and CD34 antibodies. MTT assay showed that co-culture with RVC or porous tantalum did not affect the proliferation capacity of BMSCs ($p>0.05$). After 28 co-culture days, BMSCs adhered perfectly well to the RVC and exhibited a fully spread phenotype by confocal microscope. The adhesion and spread of BMSCs on porous tantalum were better than on RVC scaffold at every time point (7d, 14d, 21d and 28d) with scanning electron microscopy. Our results show that domestic and avirulent RVC and porous tantalum have excellent biocompatibility in vitro.

IBDW2014-00114-F0042
MULTIPLE BIOMEDICAL IMAGING MODALITIES FOR SYSTEMIC EVALUATIONS OF Src siRNA DEVELOPED FOR PREVENTION OF DESTRUCTIVE REPAIR OF STEROID ASSOCIATED OSTEONECROSIS IN RABBITS

Li-zhen Zheng [a], Hui-juan Cao [b], Le Huang [a], Shi-hui Chen [a], Yi-xiang Wang [c], Tao Tang [a], Xin-luan Wang [a,b], Ling Qin [a,b]
[a]*Musculoskeletal Research Laboratory, Department of Orthopaedics and Traumatology, The Chinese University of Hong Kong, Hong Kong SAR, PR China*
[b]*Translational Medicine R&D Center, Institute of Biomedical and Health Engineering, Shenzhen Institutes of Advanced Technology, Chinese Academy of Sciences, Shenzhen, China*
[c]*Department of Imaging and Interventional Radiology, The Chinese University of Hong Kong, Hong Kong SAR, China*

Objective: We utilized multiple biomedical imaging modalities to verify our hypothesis that blocking Src activity by specific siRNA in the osteonecrosis lesion could prevent destructive repair in steroid-associated osteonecrosis (SAON) in an established rabbit model.
Methods: Fifty-one male 28-week-old rabbits were induced with destructive repair dominated SAON by pulsed injection of lipopolysaccharide (LPS) and methylprednisolone (MPS). Src siRNA was injected into proximal femur intramedullary at 2, 4, 6 weeks after induction (siSrc group, n=15). Negative siRNA served as negative control (NC group, n=15). The transfection reagent served as vehicle control (VC group, n=15). Dynamic MRI was performed on proximal femur for local intraosseous perfusion. After sacrifice at baseline (n=6) and 6 weeks post-induction, bilateral proximal femora were dissected for microCT and finite element analysis (FEA). Thereafter, bone samples were decalcified for microCT-based angiography. Local Src expression was semi-quantified by immunohistochemistry. Osteonecrotic lesion repair was classified histopathologically. The osteoblast surface (Ob.S/BS), osteoclast number (N.Oc/B.Pm) and eroded surface (ES/BS) in the repair region of subchondral bone were assessed histomorphometrically.
Results: Immunohistochemistry showed lower Src protein expression in many different kinds of cells, including vascular endothelial cells, osteoblasts, osteoclasts and osteoclast-like cells in siSrc group. Dynamic MRI showed higher vascular perfusion and inhibited vascular permeability in siSrc group. MicroCT-based angiography showed blocked stem vessels and more